Journal of Alloys and Compounds 882 (2021) 160699

Contents lists available at ScienceDirect

Journal of Alloys and Compounds

journal homepage: www.elsevier.com/locate/jalcom

Structural and magnetic properties of $SmCo_{5-X}Ni_X$ intermetallic compounds

E. Antoniou[a], G. Sempros[a], M. Gjoka[b], C. Sarafidis[a], H.M. Polatoglou[a], J. Kioseoglou[a,*]

[a] Department of Physics, Aristotle University of Thessaloniki, GR-54124 Thessaloniki, Greece
[b] Institute of Nanoscience and Nanotechnology, N.C.S.R. Demokritos, Agia Paraskevi Attikis, GR-15310 Athens, Greece

ARTICLE INFO

Article history:
Received 29 March 2021
Received in revised form 24 May 2021
Accepted 2 June 2021
Available online xxxx

Keywords:
Permanent magnets
Magnetization
Structural properties
Atomistic simulations
DFT

ABSTRACT

Modern technological applications in an extensive variety of fields require the use of Permanent Magnets (PMs). Intermetallic compounds such as $SmCo_5$ are already used as high-performance PMs. Reducing the high content of the expensive cobalt in $SmCo_5$ from low-priced transition metals can lead in a cost reduction. This study examines by computational methods the effect of substituting cobalt atoms in the crystal structure of $SmCo_5$ by nickel atoms. The aim is to specify the structure that will be stable and at the same time will maintain high values of magnetization. A series of atomistic simulations are implemented based on Density Functional Theory calculations. Various simulations are performed by considering all possible crystallographic positions of Co and Ni atoms in a $SmCo_{5-x}Ni_x$ compound. Based on energy minimization and maximizing the magnetization we pinpointed the interesting cases. An experimental implementation based on the sample with x = 1 is presented to translate the findings from atomistic simulations to realizable bulk materials. Interestingly, it is concluded that in many cases an energetically favourable atomistic configuration does not exhibit maximum magnetization. It should be noted that for the experimentally investigated case of $SmCo_4Ni$, both the energetically favourable as well as the magnetically maximum configuration have been identified.

1. Introduction

Modern technological applications in fields such as energy production, transportation and robotics [1] require the extensive use of Permanent Magnets (PMs). The importance of using PMs in practical applications is the trigger for the recent extensive research in the field. This category includes research projects in areas such as electronics, where the advancement of electronic materials is based on the evolution of PMs [2], and other areas like environmentally friendly magnetic refrigeration, which is based on the magnetocaloric effect (MCE) [3].

Intermetallic compounds based on Rare Earth Elements (REEs) are already used as high-performance PMs. A typical example of such a PM is $SmCo_5$ which has been used since the early 1960s in many applications because it displays high magnetization, large uniaxial magnetocrystalline anisotropy combined with temperature endurance [4–7].

In recent years the need to use PMs has grown due to climate change policies, a demand that cannot be met due to the limited availability of raw materials. Thus, there is need for low-cost PMs able to maintain high levels of performance. To achieve this goal the new magnetic materials must be free from expensive REEs, but also from any of the high-cost metals. This is a big challenge since the high-performance modern PMs rely on REEs for the necessary anisotropy while the transition metal sublattice provides the strong exchange interactions which deliver magnetization and temperature resistance.

In the present study we deal with the case of $SmCo_5$ for which there are two possible options. The first concerns the reduction of the concentration of Sm in the specific PM. A suitable replacement option should maintain high levels of efficiency as well as the desired cost reduction. But a second interesting option that we dealt with extensively in our research is related to the possibility of reducing the high content of cobalt by substituting Ni with some (low-priced->cheaper) transition metals. It is well known that Co is attributed to be a high criticality raw material.

Many efforts have been made to reduce the high Co content of $SmCo_5$ [8–10]. The most obvious solution is to replace Co with other transition metals such as Fe which is more abundant and less costly,

* Corresponding author.
E-mail address: sifisl@auth.gr (J. Kioseoglou).

https://doi.org/10.1016/j.jallcom.2021.160699
0925-8388/

with high atomic magnetic moment. However, the desired stable hexagonal structure is not maintained for high Fe content. Recently, an ab initio study suggested that it may be possible to partially replace Co simultaneously with Fe and Ni, suggesting that an alloy with $SmCoNiFe_3$ stoichiometry could exhibit magnetic properties suitable for applications as a PMs [11,12]. Although these claims have not yet been experimentally confirmed, the possibility of reducing the Co content to such an extent merits further study.

In the current study, ab initio computational methods were used to examine the effect of substituting cobalt atoms in the structure of $SmCo_5$ by nickel atoms. Although we are making this replacement at atomic level, the aim is to specify the structure that will be energetically stable and at the same time will maintain high values of magnetization. Nickel atoms may not have the high magnetic moment of iron atoms, but they result stable hexagonal structures and thus is more likely to maintain the energy stability of the desired structures without significantly reducing magnetization. The calculations revealed some promising compositions.

2. Computational methodology

Although a variety of well-established computational approaches has been used in comparable studies [13–17], in the present computational investigation, ab initio calculations were performed within the framework of Density Functional Theory (DFT) as implemented in the Vienna Ab-initio Simulation Package (VASP) [18,19] by the use of the plane-wave basis Projector Augmented Wave (PAW) method [20,21]. Specifically, the PAW pseudopotentials used for Sm, Co and Ni atoms came from the Perdew-Burke-Ernzerhof derivation of the Generalized Gradient Approximation (GGA-PBE) [22,23]. For total energy calculations we used the tetrahedron method with Blöchl corrections and the width of the smearing was 0.05 eV. We also used Γ-centered k-point grids. In all the relaxations the ions as well as the cell shape and volume are allowed to relax. The plane wave basis energy cut-off is 520 eV to compensate for the volume relaxations.

From the electronic configurations it appears that for Ni we have 16 valence electrons (if we consider the p electrons as valence electrons then the valence electron configuration ia $3p^6 4s^2 3d^8$) and for Co we have 9 valence electrons ($4s^2 3d^7$). According to the periodic table Sm has a total of 8 valence electrons (6f electrons and 2 s electrons). In most compounds Sm, however, adopts a valency of 3, hence 5f electrons are placed in the core, when the pseudopotential is generated (the corresponding potential can be found in the directory Sm 3). The 6th f-electron is promoted to the 5d shell. Hence as valence we have $5s^2 6s^2 5p^6 5d^1$ and a total of 11 valence electrons. Thus, the studied intermetallic compounds have many d and f elements. Classical DFT often fails to describe systems with localized d and f electrons because it provides an incorrect description of partially filled states due to self-interaction errors. An approach beyond classical DFT is needed to properly describe the behaviour of d and f electrons, therefore the DFT+U method is employed. DFT+U is a method which introduces a strong intra-atomic interaction in a screened Hartree-Fock like manner as an on-site replacement of DFT and has been used in the past for rare-earth nitrides [24]. In this work, the simplified, rotationally invariant, approach to DFT+U, introduced by Dudarev et al. [25] is used. In Dudarev's approach, the parameters U and J, which control the effective on-site Coulomb interaction and the effective on-site exchange interaction respectively, are not entered separately and only the difference U_{eff} = U-J is meaningful. U_{eff} is considered as a free parameter and is optimized according to the procedure described in [26]. Non-spherical contributions from the gradient corrections are included inside the PAW spheres, a factor essential for accurate total energies for d and f-elements if the +U approach is used.

In our DFT+U calculations we used two different sets of U parameters while J parameters were set to zero. Specifically, in the first set the U parameters 6.11 eV for Sm atoms (U_{eff} = U-J = 6.11–0 = 6.11 eV) and 4.05 eV for Co and Ni atoms (U_{eff} = U-J = 4.05–0 = 4.05 eV). The above set has been used in literature and specifically for Sm atoms the parameters used were U = 6.87 eV and J = 0.76 eV, so U_{eff} was U_{eff} = U-J = 6.87–0.76 = 6.11 eV [27] and for Co and Ni atoms the parameters used were U = 5 eV and J = 0.95 eV, so U_{eff} was U_{eff} = U-J = 5–0.95 = 4.05 eV [28]. In the second set of U parameters the corresponding values were 4.70 eV for Sm atoms and 2.22 eV for both Co and Ni atoms. Also, the U values of this parameter set have been used in similar studies, such as [29].

For PAW-PBE pseudopotentials we used the standard VASP file for Co atoms, the file named as PAW_PBE Sm_3 for Sm atoms and the file named as PAW_PBE Ni_pv for Ni atoms. The visualization of the unit cell is performed with the VESTA visualization program [30].

Several ingot samples for experimental evaluation were prepared by arc-melting constituent elements of purity better than 99.9% in Ar atmosphere. The ingots were annealed at 1200 K for 72 h in vacuum for homogenization and subsequently quenched in liquid nitrogen. X-ray diffraction plots (Cu Kα radiation) were recorded in order to confirm the produced phase.

2.1. ab initio simulations

Our investigation started with the intermetallic compounds with the largest content in Co and Ni. The $SmCo_5$ and $SmNi_5$ are described by the $CaCu_5$-type hexagonal phase of Space Group(SG) *P6/mmm* (191). In Fig. 1(a) there is a visualization of $SmCo_5$ unit cell where the red spheres represent the Sm atoms and the blue spheres the Co atoms. Similarly, in Fig. 1(b) there is a visualization of $SmNi_5$ unit cell where the silver coloured spheres are the Ni atoms. In the following Figures (Figs. 2–5) the same nuances will be maintained for the representation of the Sm, Co and Ni atoms. Also, in all visualizations the Sm–Co and Sm–Ni bonds were omitted for clarity reasons.

The results of our calculations for the magnetization (M) and the lattice constant of $SmCo_5$ and $SmNi_5$ are shown in Tables 1 and 2 respectively. The first column of both Tables shows the values of the two sets of U parameters while in the second column are the calculated magnetization values. It is obvious that the calculations of both sets of U parameters provide results for the magnetization very close to the experimental value. In fact, the calculations using the first set of U parameters result in a value for the magnetization slightly higher than the experimental one, while the calculations based on the second set of parameters result in a value slightly lower than the experimental one. Columns three and four in both Tables 1 and 2 present the calculated lattice constant parameters.

Subsequently, all possible positions of Ni atoms in the unit cell of $SmCo_5$ have been explicitly checked for all possible substitutions. For each intermetallic compound the number of possible combinations

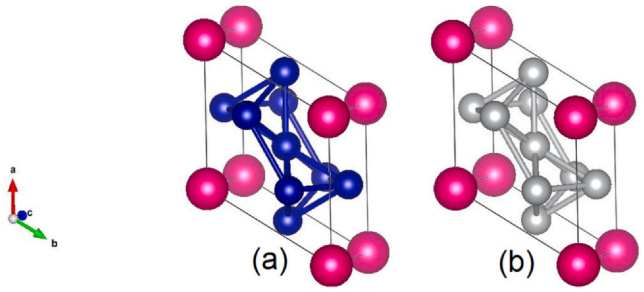

Fig. 1. Schematic illustration of the unit cell of $SmCo_5$ (a) and $SmNi_5$ (b). Red spheres represent the atoms of Sm, blue spheres the atoms of Co and silver-coloured spheres represent the atoms of Ni. For clarity, the Sm–Co bonds in (a) and Sm - Ni in (b) have been omitted.

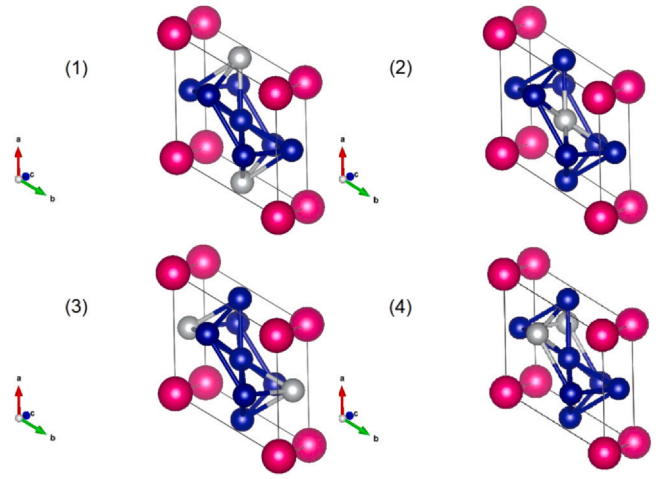

Fig. 2. Schematic illustration of four different cases of the unit cell of $SmCo_4Ni$. Cases (1), (2) & (3) are crystallographically degenerate cases.

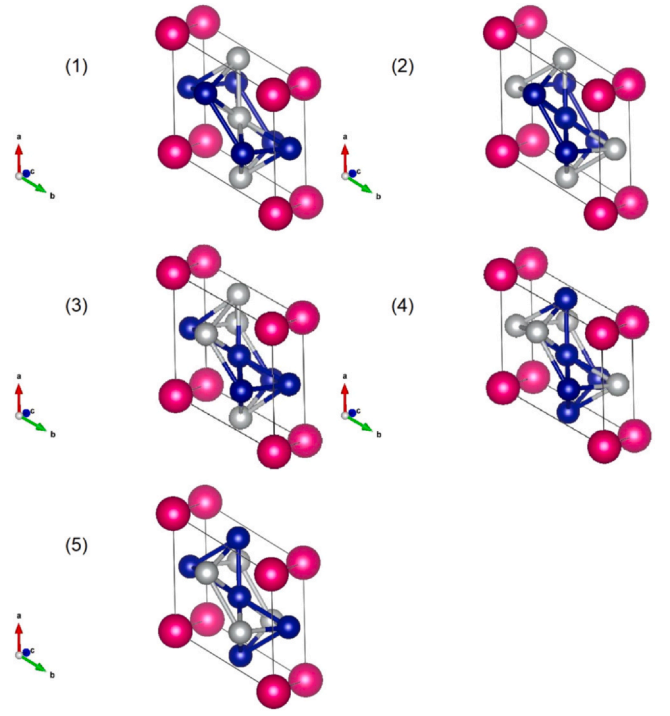

Fig. 3. Five possible cases of the unit cell of $SmCo_3Ni_2$. Cases (1) & (2) and cases (3) & (4) are crystallographically degenerate cases.

of Ni and Co atoms in the unit cell is given by the combination formula.

$$\binom{n}{r} = \frac{n!}{r!(n-r)!} \tag{1}$$

Where n is the total number of the elements of a set and r is the number of elements of a subset for which we are looking for possible combinations. In our case there is always a 6-atom unit cell and in which the sum of Ni and Co atoms is always the same and constitutes the total number of elements of our set, ie n = 5. The value of r can vary between a minimum, r = 0 for the case of $SmCo_5$ and a maximum, r = 5 for the case of $SmNi_5$. From all the possible combinations may exist for each intermetallic compound considering $1 \le r \le 4$, few are proved to be crystallographically degenerate owing to the symmetry operations of the unit cell.

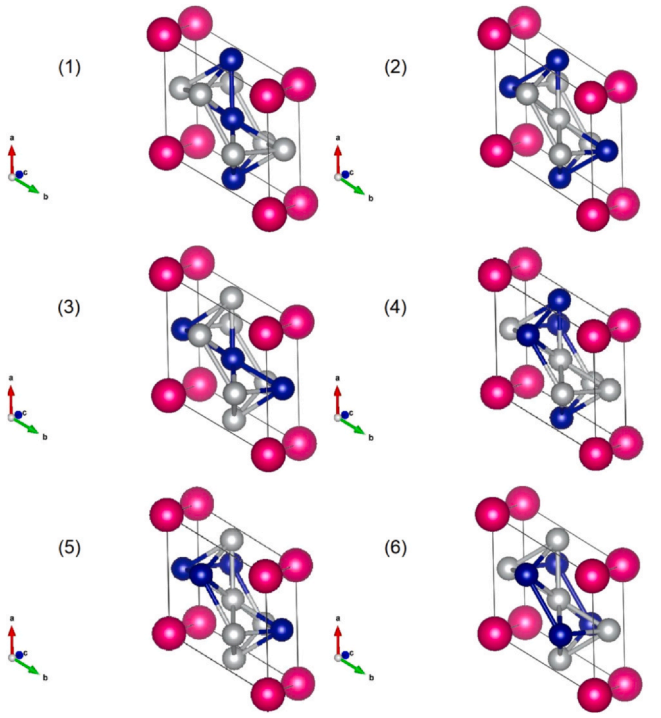

Fig. 4. Schematic illustration of six different cases of the unit cell of $SmCo_2Ni_3$. Cases (1), (2) & (3) and (4) & (5) are crystallographically degenerate cases.

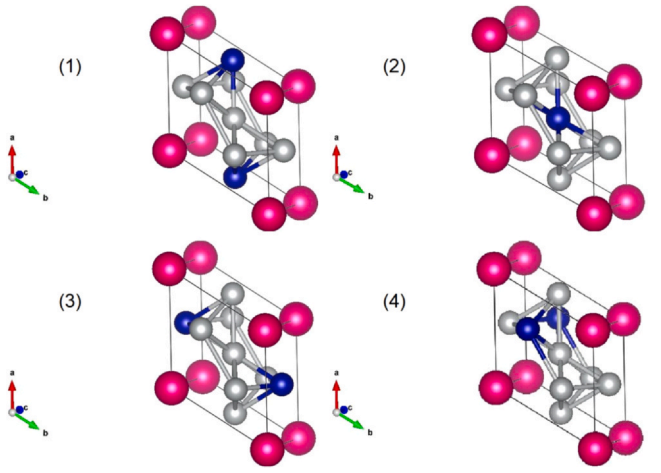

Fig. 5. Schematic illustration of four different cases of the unit cell of $SmCoNi_4$. Cases (1), (2) & (3) are crystallographically degenerate cases.

Table 1
$SmCo_5$ Intermetallic Compound.

DFT+U	M (μ_B)	a (Å)	c (Å)
Sm: 6.11 Co, Ni: 4.05	9.383	5.252	3.844
Sm: 4.70 Co, Ni: 2.22	8.523	5.071	3.867
Experimental*	8.900	5.002	3.961

Note. * In the last line of the Table there are the experimental values of magnetization and lattice constant parameters [31].

2.2. $SmCo_4Ni$

Starting to replace Co atoms with Ni atoms in the $SmCo_5$ unit cell structure we first studied the unit cell of $SmCo_4Ni$ intermetallic compound. In the unit cell consisting of six atoms there is now one Ni atom. Using the combination formula (n = 5 and r = 1) we found that there are five possible combinations for the arrangement of Ni

Table 2
$SmNi_5$ Intermetallic Compound.

DFT+U	M (μ_B)	a (Å)	c (Å)
Sm: 6.11 Co, Ni: 4.05	2.761	4.906	3.942
Sm: 4.70 Co, Ni: 2.22	1.942	4.900	3.945
Experimental*	0.850	4.920	3.966

Note. * In the last line of the Table there are the experimental values of magnetization and lattice constant parameters [32].

and Co atoms in the unit cell. In Fig. 2 there is a visualization of four different possible cases (cases 1, 2, 3 & 4) for the arrangement of the atoms in the unit cell of $SmCo_4Ni$. In their representation, we have presented them having the same orientation. As it turned out considering the translational and rotational symmetry of the unit cell, cases (1), (2) & (3) in Fig. 2 are crystallographically degenerate cases.

In Table 3 there are the results of our calculations using the first set of U parameters. That is U = 6.11 eV for Sm atoms and U = 4.05 eV for Co and Ni atoms. For each of four cases in columns 2, 3 and 4 the difference in energy (ΔE) in relation to the case with the least energy, the magnetization (M) and the difference in magnetization (ΔM) in relation to the case with the highest magnetization are presented respectively. Columns 5 and 6 present the percentage differences in the lattice parameters a and c for each case in relation to the lattice parameters of $SmCo_5$ which provide an indication of the deformation of the unit cell.

Our calculations showed that for this set of U parameters the energetically favourable case is case number 1. The same case is also the case with the maximum magnetization.

For the same intermetallic compound but for the second set of U parameters (U = 4.70 eV for Sm atoms and U = 2.22 eV for Co and Ni atoms) Table 4 shows the results of our calculations. According to these calculations the energetically favourable case is again case number 1 but now the case with the maximum magnetization is case number 4.

2.3. $SmCo_3Ni_2$

The unit cell of $SmCo_3Ni_2$ is a 6-atom unit cell with 2 Ni atoms. With the use of the combination formula (n = 5 and r = 2) we found that there are ten possible combinations for the arrangement of Ni and Co atoms in the unit cell. After the initial identification of identical cases five different possible cases (cases 1, 2, 3, 4 & 5) for the arrangement of the Ni and Co atoms in the unit cell left. In Fig. 3 there is an illustration of these five different possible cases. In view of the translational and rotational symmetry of the unit cell, we found that case (1) is crystallographically degenerated with case (2) and the same is found for case (3) which is crystallographically degenerated with case (4).

In Table 5 there are the results for the calculations with the use of the set of U parameters with the higher values for $SmCo_3Ni$. It is obvious that case 3 is the energetically favourable case and also has the maximum magnetization.

Table 3
Different cases of $SmCo_4Ni$ Intermetallic Compound with DFT+U 6.11 for Sm and 4.05 for Co & Ni.

Cases	ΔE (eV)	M (μ_B)	ΔM (μ_B)	Δa/a (%)	Δc/c (%)
1	0.000[a]	7.918	0.000[b]	0.51	0.80
4	0.494	7.902	-0.021	-1.99	4.07

Notes: The differences in energy (ΔE) and magnetization (ΔM) for each case were calculated with respect to the case with the least energy and the highest magnetization respectively. Percentage differences in the lattice parameters *a* and *c* for each case were calculated with respect to the lattice parameters of $SmCo_5$.
[a] Case with the minimum energy.
[b] Case with the maximum magnetization.

Table 4
Different cases of $SmCo_4Ni$ Intermetallic Compound with DFT+U 4.70 for Sm and 2.22 for Co & Ni.

Cases	ΔE (eV)	M (μ_B)	ΔM (μ_B)	Δa/a (%)	Δc/c (%)
1	0.000*	7.133	-0.182	1.22	1.53
4	0.188	7.315	0.000**	-1.61	2.36

Notes: As in Table 3
* Case with the minimum energy.
** Case with the maximum magnetization.

The calculations with the use of the set of U parameters with the smaller values for $SmCo_3Ni_2$ are shown in Table 6. According to these calculations case 3 maintains as the energetically favourable case while case 5 has the maximum magnetization.

2.4. $SmCo_2Ni_3$

The intermetallic compound of $SmCo_2Ni_3$ has three Ni atoms in its unit cell. With the use of the combination formula (n = 5 and r = 3) we found that there are ten possible combinations for the arrangement of Ni and Co atoms in the unit cell. After the initial identification and the removal of identical cases, six different possible cases (cases 1, 2, 3, 4, 5 & 6) for the arrangement of the Ni and Co atoms in the unit cell left. In Fig. 4 there is the visualization of these six different possible cases of the arrangement of the Ni and Co atoms in the unit cell. Considering the translational and rotational symmetry of the unit cell we found that cases (1), (2) and (3) are crystallographically degenerate cases. The same is valid for cases (4) and (5).

In Table 7 there are the results of our calculations using the first set of U parameters, with U = 6.11 eV for Sm atoms and U = 4.05 eV for Co and Ni atoms.

Our calculations showed that for this set of U parameters the energetically favourable case is case number 1 while case number 6 is the case with the maximum magnetization.

The calculations with the use of U = 4.70 eV for Sm atoms and 2.22 eV for Co and Ni atoms for the $SmCo_2Ni_3$ intermetallic compound are presented in Table 8. Case 1 is the energetically favourable case and also has the maximum magnetization.

2.5. $SmCoNi_4$

$SmCoNi_4$ is the last structure studied and has a 6-atom unit cell with four Ni atoms. Using the combination formula (n = 5 and r = 4) we found that there are five possible combinations for the arrangement of Ni and Co atoms in the unit cell. An identical case was initially identified and removed and so on in Fig. 5 there is a visualization of four different possible cases (cases 1, 2, 3 & 4) for the arrangement of the atoms in the unit cell of $SmCoNi_4$. From these cases (1), (2) and (3) are crystallographically degenerate cases as evidenced by the translational and rotational symmetry of the unit cell.

The results of our calculations for $SmCoNi_4$ with the use of the first set of U parameters (U = 6.11 eV for Sm atoms and U = 4.05 eV for Co and Ni atoms) are shown in Table 9. These calculations point as

Table 5
Different cases of $SmCo_3Ni_2$ Intermetallic Compound with DFT+U 6.11 for Sm and 4.05 for Co & Ni.

Cases	ΔE (eV)	M (μ_B)	ΔM (μ_B)	Δa/a (%)	Δc/c (%)
1	0.156	6.332	-0.558	-4.39	3.99
3	0.000*	6.890	0.000**	-0.87	3.90
5	0.728	6.648	-0.242	-5.59	7.97

Notes: As in Table 3
* Case with the minimum energy.
** Case with the maximum magnetization.

Table 6
Different cases of $SmCo_3Ni_2$ Intermetallic Compound with DFT+U 4.70 for Sm and 2.22 for Co & Ni.

Cases	ΔE (eV)	M (μ_B)	ΔM (μ_B)	Δa/a (%)	Δc/c (%)
1	0.146	5.948	-0.165	-1.84	0.99
3	0.000*	5.959	-0.154	-0.44	1.20
5	0.136	6.113	0.000**	-3.66	5.14

Notes: As in Table 3
* Case with the minimum energy.
** Case with the maximum magnetization.

Table 7
Different cases of $SmCo_2Ni_3$ Intermetallic Compound with DFT+U 6.11 for Sm and 4.05 for Co & Ni.

Cases	ΔE (eV)	M (μ_B)	ΔM (μ_B)	Δa/a (%)	Δc/c (%)
1	0.000*	5.444	-0.212	-3.31	4.22
4	0.309	5.326	-0.330	-4.41	3.12
6	1.376	5.656	0.000**	-4.84	1.80

Notes: As in Table 3
* Case with the minimum energy.
** Case with the maximum magnetization.

Table 8
Different cases of $SmCo_2Ni_3$ Intermetallic Compound with DFT+U 4.70 for Sm and 2.22 for Co & Ni.

Cases	ΔE (eV)	M (μ_B)	ΔM (μ_B)	Δa/a (%)	Δc/c (%)
1	0.000*	4.986	0.000**	-0.77	3.23
4	0.212	4.972	-0.014	-2.87	1.70
6	0.567	4.711	-0.275	-3.07	2.81

Notes: As in Table 3
* Case with the minimum energy.
** Case with the maximum magnetization.

the energetically favourable the first case while the case with the maximum magnetization is case 4.

In Table 10 the results of the calculations with the smaller values of the U parameters are presented. Case 1 is simultaneously the energetically favourable and the case with the maximum magnetization.

Summarizing the above results one can observe that although the calculations with the two different sets of U parameters give different values for the energy, that does not affect the energy ordering of the compounds. Thus, we can conclude which is the energetically favourable case for every content of Ni atoms. In addition, the first set of U parameters always leads to higher magnetization results than those of the second set. This is in line with our initial observation about $SmCo_5$ where the first set gives slightly higher magnetization values than the experimental ones, while the second set gives slightly lower values. In Fig. 6 there is a plot of the maximum magnetization in every intermetallic compound studied. As shown in the diagram an increase in the number of Ni atoms in the unit cell leads to a linear decrease in Magnetization and this observation applies to the calculations with both sets of U parameters.

Table 9
Different cases of $SmCoNi_4$ Intermetallic Compound with DFT+U 6.11 for Sm and 4.05 for Co & Ni.

Cases	ΔE (eV)	M (μ_B)	ΔM (μ_B)	Δa/a (%)	Δc/c (%)
1	0.000*	4.028	-0.031	-7.02	5.61
4	0.589	4.059	0.000**	-5.63	2.09

Notes: As in Table 3
* Case with the minimum energy.
** Case with the maximum magnetization.

Table 10
Different cases of $SmCoNi_4$ Intermetallic Compound with DFT+U 4.70 for Sm and 2.22 for Co & Ni.

Cases	ΔE (eV)	M (μ_B)	ΔM (μ_B)	Δa/a (%)	Δc/c (%)
1	0.000*	3.621	0.000**	-3.86	2.65
4	0.279	3.533	-0.088	-2.67	1.59

Notes: As in Table 3
* Case with the minimum energy.
** Case with the maximum magnetization.

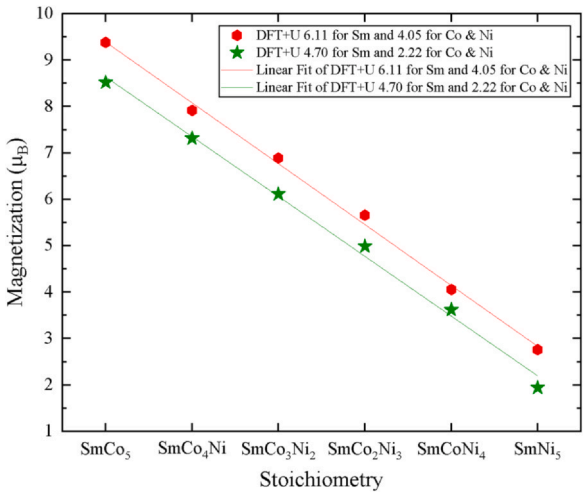

Fig. 6. The maximum Magnetization of every intermetallic compound for both sets of U parameters.

2.6. Non-collinear (NCL) simulations

In the previous section the results for the magnetization came from the use of collinear calculations, which are based on a simplified theoretical model where the directions of the atomic spin are set to be either co-parallel or anti-parallel. This approximation provides relatively accurate calculations, short simulation time and simple implementation. Another approach to calculating magnetization can be given by noncollinear calculations where the magnetization density is considered as a continuous vector variable of position and has been proved suitable for the vast majority of the materials systems such as crystalline and amorphous semiconductors, simple liquids and especially for transition metals [33]. Hence, to complete our study we proceeded to conduct noncollinear calculations for each of the intermetallic compound studied above.

The results of the non-collinear calculations, using DFT+U 6.11 for Sm and 4.05 for Co and Ni, indicated that different cases exhibit maximum magnetization than those indicated by the collinear calculations with the same set of U parameters. In fact, the atomistic models of maximum magnetization are now identical to those proposed by the collinear calculations made with DFT+U 4.70 for Sm and 2.22 for Co and Ni.

Table S1[1] presents both the magnetizations resulting from collinear and non-collinear calculations for each case of $SmCo_4Ni$ intermetallic compound. The corresponding values of magnetizations for $SmCo_3Ni_2$ are shown in Table S2. Tables S3 and S4 show the results of the collinear and non-collinear calculations for cases of $SmCo_2Ni_3$ and $SmCoNi_4$ intermetallic compound respectively. The Tables S1–S4 are calculated by DFT+U 6.11 for Sm and 4.05 for Co & Ni.

[1] The Tables S1–S6 are presented in the Supplementary Information document.

In order to focus on the cases indicated as cases of maximum magnetization from the non-collinear calculations, Table S5 shows the values of maximum magnetization calculated by non-collinear calculations for each intermetallic compound with DFT+U 6.11 for Sm and 4.05 for Co & Ni as well as the corresponding magnetization values of the same cases calculated by collinear calculations.

Table S6 shows the values of maximum magnetization calculated by collinear and non-collinear calculations for each intermetallic compound with DFT+U 4.70 for Sm and 2.22 for Co & Ni.

Remarkably, the results of the non-collinear calculations, using DFT+U 4.70 for Sm and 2.22 for Co and Ni, indicate that the cases of maximum magnetization are the same with those indicated by the collinear calculations with the same set of U parameters. Moreover, using non-collinear calculations both sets of U parameters result in the same cases of maximum magnetization for each intermetallic compound that has been studied in our research. This match did not exist in the results of the collinear calculations.

The aforementioned analysis leads to the conclusion that the set of U parameters, 4.70 for Sm and 2.22 for Co and Ni, is the most reliable set for $SmCo_{5-x}Ni_x$.

The following Fig. 7 was made using the data of Tables S5 and S6. It becomes clear that even using non-collinear calculations the values of the maximum magnetization calculated from the set with the highest values of U parameters are still greater than those resulting from the set with the lowest U values. It is recalled that our research carried out using collinear calculations had reached at the same conclusion.

3. Experimental evaluation

Concerning the experimental evaluation, we have chosen to synthesize the $SmCo_4Ni$ stoichiometry in order to detect which arrangement is more favourable. There are few experimental descriptions of $SmCo_4Ni$ samples [34]. In Fig. 8 the X-ray diffraction plots for both as-casted and annealed samples are presented. Both diffractograms are practically the same, with minor differences in some relative peak intensities due to the most ordered and arranged structure after the annealing. According to a Rietveld analysis the typical hexagonal $CaCu_5$-type phase is formed (SG 191, *P6/mmm*) with unit cell parameters a = b = 0.4972(2) nm, c = 0.3981(1) nm, c/a = 0.801 and V = 0.0852(5) nm^3 for the as-casted and a = b = 0.4975(1) nm, c = 0.3980(1) nm, c/a = 0.800 and V = 0.0853(2) nm^3 for the annealed; these values are typical for the $SmCo_5$ phase [35,36]. With X-ray diffraction is difficult to identify if there is

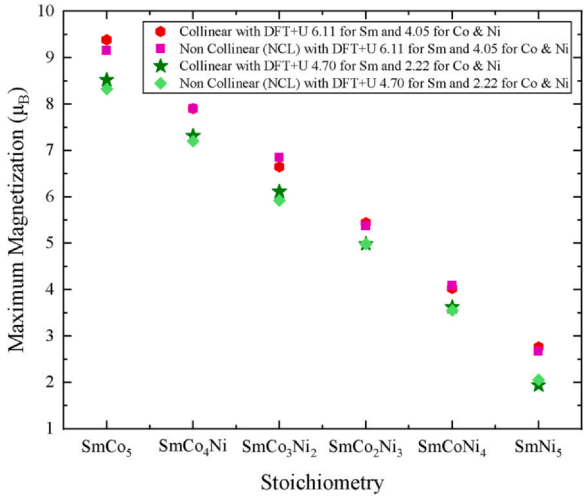

Fig. 7. The maximum magnetization of every intermetallic compound for both sets of U parameters as calculated by collinear and non-collinear simulations.

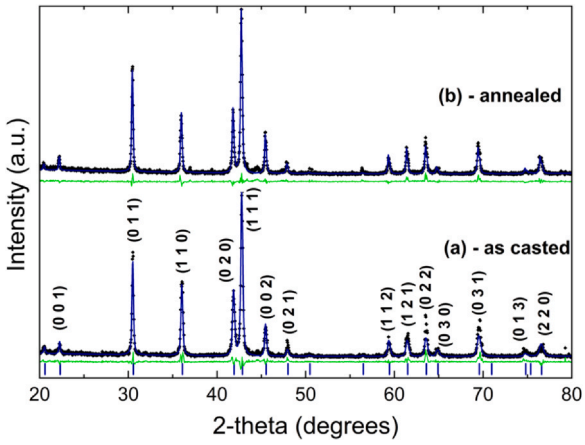

Fig. 8. X-ray diffraction plots for $SmCo_4Ni$ powder (a) as casted and (b) annealed.

preference in Ni replacement for Co. By assuming that Ni tends to avoid the Co-only "Kagome" layers (3 g positions) and thus prefer the Sm_4Co_2 layers (2c positions) a very small improvement in the fit was observed. It is concluded that at temperatures up to 1200 K the lower c/a phase is more preferable and possibly the stabilization of higher c/a with the enhanced magnetic properties requires a slightly different stoichiometry; higher annealing temperature produces other variants [36].

Samples with SmCo4Ni stoichiometry (x = 1) were prepared for experimental evaluation; it is well known that $SmNi_5$ is not suitable for applications as PM and it unlikely that replacement of Co by Ni in large amounts will produce phases with suitable structural and magnetic properties. Additionally, the complex physics of these intermetallic systems require the experimental validation of the ab-initio calculations especially in the case of confirmation or optimization of various parameters which affect the simulations. The specific experimental stoichiometry was a safe choice with the least amount of Ni in order to confirm the calculations and acquire information about the physics of this system; further Co reduction in the system probably requires the study of more complex stoichiometries and thus the good knowledge of the system is important.

4. Discussion

The use of permanent magnets in modern technological applications is extensive. Limited availability and high cost of the necessary raw materials in manufacturing of permanent magnets have increased the need to develop innovative materials. Therefore, the search for cheaper and more efficient magnetic materials is necessary for the maintenance and development of these applications. Reducing the cobalt content in the $SmCo_5$ unit cell by substituting cobalt atoms with nickel atoms could lead to a low-cost permanent magnet.

It is evident that magnetization is an important parameter in the evaluation of a material's usefulness in applications as a permanent magnet; it is also well expected that replacement of Co by Ni will probably reduce the magnetization. In general, other, intrinsic and extrinsic parameters are also important from applications' scope while price and especially the supply criticality are often a defining parameter in industrial design and hence the incorporation of Ni in $SmCo_5$ structure is under intense investigation[11,12,34,37–43]. In addition, even the complete substitution of Co by Ni is attracted the attention [32,44–47]. Co is considered a material with high supply risk (e.g. [48–50]). Also, it is well known that in the base materials used in permanent magnets there is a performance gap [1] between expensive, high performing materials and cheaper, low performing counterparts. Several applications would benefit from materials

within this gap, less expensive but with a compromise in performance. However, the present work's scope is not directly related to the suggestion of a Ni-doped $SmCo_5$ phase as a material definitely suitable for applications, with an overall merit (including price and supply safety) superior to all existing ones. The main focus of the current investigation is to contribute in the understanding of the complex nature of the physics within the system, the interactions that affect primarily the structural characteristics and the stability and additionally the magnetic properties of the phase. It is well known [5] that the number of transition metal *3d* electrons is definitely related to the stability and the magnetic properties of the system and that by increasing transition metal electrons, Ni content in our case, improves the stability of the material. By testing and improving the ab initio calculation parameters and gaining further knowledge for the 1:5 phase future studies will possibly determine materials with more suitable overall merit for applications. The current study contributes towards this scope and will assist other researchers in the field to target new stoichiometries more efficiently, considering the obvious fact that ab-initio methods are easier and energy efficient in implementation than empirical experimental evaluation.

5. Conclusions

Structural stability and magnetization of $SmCo_{5-x}Ni_x$ intermetallics is elucidated by means of ab initio calculations. It is known that full Co replacement by Ni does not produce a material with suitable properties for PM applications, however the fine tuning of stoichiometry may lead to a desired combination of performance vs raw materials' criticality. Understanding and optimizing ab-initio simulation parameters is important for studying more complicated stoichiometries. Experimental evaluation for x = 1 compound confirmed the predicted structure. The computational implementation is based on investigating crystallographically possible atomistic configurations for each x in $SmCo_{5-x}Ni_x$. Collinear and non-collinear DFT based calculations are performed using two different sets of U parameters. Focusing on the energy and magnetization of the intermetallic compounds $SmCo_{5-x}Ni_x$ a variety of outcomes are emerged.

Concerning the energetical structural stability of the investigated cases, it is resolved that both sets of U parameters concluded on the same energy hierarchy; consequently, both sets are able to determine the energetically preferable cases for each Ni content.

Magnetization decreases linearly with Ni for both sets of U parameters and for both types of calculations (collinear and non-collinear). Moreover, it is established that the magnetization values provided by the first set of parameters U (6.11 for Sm and 4.05 for Co & Ni) are always greater than the values provided by the second set (U = 4.70 eV for Sm atoms and U = 2.22 eV for Co & Ni atoms). The crystallographic structural model with the highest magnetization differs for the two sets of U parameters for collinear calculations. With non-collinear calculations both sets of U's provide the same model as the one with the highest magnetization. Either collinear and non-collinear calculations with the second set of the U parameters (U = 4.70 eV for Sm atoms and U = 2.22 eV for Co & Ni atoms) conclude at the same structural models as maximum magnetization cases. The first set of U (6.11 for Sm and 4.05 for Co & Ni) results in magnetization values larger than the experimental ones, while the second set of U (4.70 for Sm and 2.22 for Co & Ni) results in smaller magnetization values. In view of the aforementioned conclusions, it is established that the set of U parameters, 4.70 for Sm and 2.22 for Co and Ni, is the most reliable set for $SmCo_{5-x}Ni_x$.

One of the most important conclusions the $SmCo_{5-x}Ni_x$ compounds is that in many cases the energetically favourable atomistic configuration does not exhibit the maximum magnetization. Hence, it is obvious that the atomistic model with the maximum magnetization requires more energy to be formed, that deviation from the energetically favourable and therefore highly symmetrical unit cell leads to atomistic configurations with maximum magnetization.

CRediT authorship contribution statement

E. Antoniou: performed the simulations described in the work and analyzed the results; **G. Sempros, M. Gjoka, C. Sarafidis**: performed the experiments presented in the manuscript and conducted the analysis of the experimental results; **H.M. Polatoglou, J. Kioseoglou**: designed and interpreted the simulations; All authors contributed to the Writing - review & editing.

Data Availability

The datasets generated during and/or analysed during the current study are available in the Zenodo repository, http://doi.org/10.5281/zenodo.4742473. Supplementary Information is available in the online version of the paper.

Declaration of Competing Interest

The authors declare that they have no known competing financial interests or personal relationships that could have appeared to influence the work reported in this paper.

Acknowledgements

"This research is co-financed by Greece and the European Union (European Social Fund- ESF) through the Operational Programme "Human Resources Development, Education and Lifelong Learning 2014–2020" in the context of the project "Ab initio computational investigation and experimental growth & characterization of advanced materials for permanent magnets." (MIS 5047849)."

.

This work was supported by computational resources granted from the Greek Research & Technology Network (GRNET) in the National HPC facility 'ARIS' under the project NOUS (pr010034).

Appendix A. Supporting information

Supplementary data associated with this article can be found in the online version at doi:10.1016/j.jallcom.2021.160699.

References

[1] O. Gutfleisch, M.A. Willard, E. Brück, C.H. Chen, S.G. Sankar, J.P. Liu, Magnetic materials and devices for the 21st century: stronger, lighter, and more energy efficient, Adv. Mater. 23 (7) (2011) 821–842, https://doi.org/10.1002/adma.201002180

[2] Deqing Zhang, Junye Cheng, Jixing Chai, Jiji Deng, Ran Ren, Yang Su, Hao Wang, Chunqing Ma, Chun-Sing Lee, Wenjun Zhang, Guang-Ping Zheng, Maosheng Cao, Magnetic-field-induced dielectric behaviors and magneto-electrical coupling of multiferroic compounds containing cobalt ferrite/barium calcium titanate composite fibers, J. Alloy. Compd. 740 (2018) 1067–1076, https://doi.org/10.1016/j.jallcom.2018.01.081

[3] Junye Cheng, Tian Li, Sana Ullah, Feng Luo, Hao Wang, Ming Yan, Guangping Zheng, Giant magnetocaloric effect in nanostructured Fe-Co-P amorphous alloys enabled through pulse electrodeposition, Nanotechnology 31 (38) (2020) 385704, https://doi.org/10.1088/1361-6528/ab9971

[4] A.M. Gabay, G.C. Hadjipanayis, Application of mechanochemical synthesis to manufacturing of permanent magnets, JOM 67 (6) (2015) 1329–1335, https://doi.org/10.1007/s11837-015-1426-4

[5] A.M. Gabay, X.C. Hu, G.C. Hadjipanayis, Preparation of YCo_5, $PrCo_5$ and $SmCo_5$ anisotropic high-coercivity powders via mechanochemistry, J. Magn. Magn. Mater. 368 (2014) 75–81, https://doi.org/10.1016/j.jmmm.2014.05.014

[6] B. Balamurugan, R. Skomski, D.L. Roy, G.C. Hadjipanayis, J.E. Shield, D.J. Sellmyer, Cluster synthesis, direct ordering and alignment of rare-earth transition- metal nanomagnets, Energy Technology 2012: Carbon Dioxide Management and Other Technologies, (2012) pp. 382-390. DOI: 10.1002/9781118365038.ch44.

[7] Zhaoguo Qiu, J. Ping Liu, Hongya Yu, Narayan Poudyal, Guangbing Han, Dechang Zeng, Yuan Hong, Atomic diffusion and microstructure of SmCo5 multilayers with high coercivity, J. Alloy. Compd. 733 (2018) 45–52, https://doi.org/10.1016/j.jallcom.2017.10.286

[8] D.W. Hu, M. Yue, J.H. Zuo, R. Pan, D.T. Zhang, W.Q. Liu, J.X. Zhang, Z.H. Guo, W. Li, Structure and magnetic properties of bulk anisotropic $SmCo_5$/α-Fe nanocomposite permanent magnets prepared via a bottom up approach, J. Alloy. Compd. 538 (2012) 173–176, https://doi.org/10.1016/j.jallcom.2012.05.079

[9] Tetsuji Saito, Daisuke Nishio-Hamane, High-coercivity $SmCo_5$/α-Fe nanocomposite magnets, J. Alloy. Compd. 735 (2018) 218–223, https://doi.org/10.1016/j.jallcom.2017.11.060

[10] L. Bian, Y. Li, X. Han, J. Cheng, X. Qin, Y. Zhao, J. Sun, Phys. B Condens. Matter 531 (2018) 1–8, https://doi.org/10.1016/j.physb.2017.12.019

[11] P. Söderlind, A. Landa, I.L.M. Locht, D. Åberg, Y. Kvashnin, M. Pereiro, M. Däne, P.E.A. Turchi, V.P. Antropov, O. Eriksson, Prediction of the new efficient permanent magnet $SmCoNiFe_3$, Phys. Rev. B 96 (2017) 100404, https://doi.org/10.1103/PhysRevB.96.100404

[12] A. Landa, P. Söderlind, D. Parker, D. Åberg, V. Lordi, A. Perron, P.E.A. Turchi, R.K. Chouhan, D. Paudyal, T.A. Lograsso, Thermodynamics of $SmCo_5$ compound doped with Fe and Ni: an ab initio study, J. Alloy. Compd. 765 (2018) 659–663.

[13] O. Grånäs, I. Di Marco, P. Thunström, L. Nordström, O. Eriksson, T. Björkman, J.M. Wills, Charge self-consistent dynamical mean-field theory based on the full-potential linear muffin-tin orbital method: methodology and applications, Comput. Mater. Sci. 55 (2012) 295–302, https://doi.org/10.1016/j.commatsci.2011.11.032

[14] X.B. Liu, Z. Altounian, Magnetic moments and exchange interaction in Sm(Co,Fe)5 from first-principles, Comput. Mater. Sci. 50 (2011) 841–846, https://doi.org/10.1016/j.commatsci.2010.10.019

[15] B. Minisini, P. Bonnaud, Q.A. Wang, F. Tsobnang, DFT evaluation of thermo-mechanical properties of scheelite type $MLiF_4$ (M=La, Ce, Pr, Nd, Pm, Sm, Gd, Tb, Dy, Ho, Er, Tm, Lu, Comput. Mater. Sci. 42 (1) (2008) 156–160, https://doi.org/10.1016/j.commatsci.2007.07.001

[16] S. Yehia, S.H. Aly, A.E. Aly, Electronic band structure and spin-density maps of $SmCo_5$, Comput. Mater. Sci. 41 (4) (2008) 482–485, https://doi.org/10.1016/j.commatsci.2007.05.004

[17] R.F. Sabirianov, A. Kashyap, R. Skomski, S.S. Jaswal, D.J. Sellmyer, La Crosse viral infection in hospitalized pediatric patients in Western North Carolina, Hosp. Pediatr. 2 (2012) 235–242, https://doi.org/10.1063/1.1792791

[18] G. Kresse, J. Furthmüller, Efficient iterative schemes for ab-initio total energy calculations using a plane-wave basis set, Phys. Rev. B 54 (16) (1996) 11169–11186.

[19] G. Kresse, G, D. Joubert, From ultrasoft pseudopotentials to the projector augmented-wave method, Phys. Rev. B 59 (3) (1999) 1758–1775.

[20] P.E. Blöchl, Projector augmented-wave method, Phys. Rev. B Condens. Matter 50 (1994) 17953–17979, https://doi.org/10.1103/PhysRevB.50.17953

[21] G. Kresse, D. Joubert, From ultrasoft pseudopotentials to the projector augmented-wave method, Phys. Rev. B 59 (1999) 1758–1775, https://doi.org/10.1103/PhysRevB.59.1758

[22] J.P. Perdew, K. Burke, M. Ernzerhof, Generalized gradient approximation made simple, Phys. Rev. Lett. 77 (1996) 3865–3868, https://doi.org/10.1103/PhysRevLett.77.3865

[23] J.P. Perdew, K. Burke, M. Ernzerhof, Generalized gradient approximation made simple, Phys. Rev. Lett. 78 (1997) 1396, https://doi.org/10.1103/PhysRevLett.78.1396 (1396–1396).

[24] P. Larson, Walter R.L. Lambrecht, A. Chantis, M. van Schilfgaarde, Electronic structure of rare-earth nitrides using theLSDA+Uapproach: Importance of allowing 4f orbitals to break the cubic crystal symmetry, Phys. Rev. B 75 (2007) 045114, https://doi.org/10.1103/PhysRevB.75.045114

[25] S.L. Dudarev, G.A. Botton, S.Y. Savrasov, C.J. Humphreys, A.P. Sutton, Electron-energy-loss spectra and the structural stability of nickel oxide: an LSDA+U study, Phys. Rev. B. 57 (1998) 1505–1509, https://doi.org/10.1103/PhysRevB.57.1505

[26] B. Hourahine, S. Sanna, B. Aradi, C. Kohler, T. Frauenheim, A theoretical study of erbium in GaN, Phys. B Condens. Matter 376–377 (2006) 512–515, https://doi.org/10.1016/j.physb.2005.12.130

[27] A.L. Kozub, A.B. Shick, F. Máca, J. Kolorenč, A.I. Lichtenstein, Electronic structure and magnetism of samarium and neodymium adatoms on free-standing graphene, Phys. Rev. B 94 (2016) 125113, https://doi.org/10.1103/PhysRevB.94.125113

[28] M. Sieberer, J. Redinger, P. Mohn, Electronic and magnetic structure of cuprous oxide Cu_2O doped with Mn, Fe, Co, and Ni: a density-functional theory study, Phys. Rev. B 75 (2007) 035203, https://doi.org/10.1103/PhysRevB.75.035203

[29] D. van der Marel, G.A. Sawatzky, Electron-electron interaction and localization in d and f transition metals, Phys. Rev. B Condens. Matter 37 (1988) 10674–10684, https://doi.org/10.1103/PhysRevB.37.10674

[30] K. Momma, F. Izumi, VESTA 3 for three-dimensional visualization of crystal, volumetric and morphology data, J. Appl. Crystallogr. 44 (2011) 1272–1276, https://doi.org/10.1107/S0021889811038970

[31] Z. Tie-song, J. Han-min, G. Guang-hua, H. Xiu-feng, C. Hong, Magnetic properties of R ions in RCo5 compounds (R=Pr, Nd, Sm, Gd, Tb, Dy, Ho, and Er), Phys. Rev. B Condens. Matter 43 (10) (1991) 8593–8598, https://doi.org/10.1103/physrevb.43.8593

[32] K. Nouri, M. Jemmali, S. Walha, K. Zehani, A. Ben Salah, L. Bessais, Structural, atomic Hirschfeld surface, magnetic and magnetocaloric properties of $SmNi_5$ compound, J. Alloy. Compd. 672 (2016) 440–448, https://doi.org/10.1016/j.jallcom.2016.02.142

[33] D. Hobbs, G. Kresse, J. Hafner, Fully unconstrained noncollinear magnetism within the projector augmented-wave method, Phys. Rev. B 62 (2000) 11556–11570, https://doi.org/10.1103/PhysRevB.62.11556

[34] M.T. Mikhov, W. Gong, G.C. Hadjipanayis, La Crosse viral infection in hospitalized pediatric patients in Western North Carolina, Hosp. Pediatr. 2 (2012) 235–242, https://doi.org/10.1063/1.338753

[35] X. Chi, Y. Li, D.Q. Er, X.H. Han, X.L. Duan, J.B. Sun, C.X. Cui, Oxygenation of frog gastric mucosa in vitro, Adv. Mater. Sci. Eng. 2018 (2018), https://doi.org/10.1155/2018/6457534

[36] Y. Khan, On the crystal structures of the R_2Co_{17} intermetallic compounds, Acta Crystallogr. B Struct. Crystallogr. Cryst. Chem. 29 (1973) 2502–2507, https://doi.org/10.1107/S0567740873006928

[37] H.-W. Wang, S. Wang, Y.-F. Cao, T.-Y. Liu, J.-B. Sun, Y. Zhang, Structure and magnetic properties of alnico alloy doped $SmCo_5$–Cu ribbons, J. Magn. Magn. Mater. 528 (2021) 167821, https://doi.org/10.1016/j.jmmm.2021.167821

[38] B. Belan, D. Kowalska, M. Manyako, M. Dzevenko, Y. Kalychak, Single-crystal investigation of the compound $SmNi_{5.2}Mn_{6.8}$, Z. Naturforsch. Sect. B J. Chem. Sci. 75 (3) (2020) 303–307, https://doi.org/10.1515/znb-2019-0181

[39] L.-P. Bian, Y. Li, X.-H. Han, J.-Y. Cheng, X.-N. Qin, Y.-Q. Zhao, J.-B. Sun, Effect of multi-element addition of Alnico alloying elements on structure and magnetic properties of $SmCo_5$ -based ribbons, Phys. B Condens. Matter 531 (2018) 1–8, https://doi.org/10.1016/j.physb.2017.12.019

[40] M. López, R.V. Mangalaraja, J.A. Jiménez, Microstructure and magnetic properties of $Cu_{90-x}Co_{10}Ni_x$–7.5% SmCo5composite alloys prepared by mechanical alloying and hot pressing, Powder Metall. 60 (1) (2017) 33–41, https://doi.org/10.1080/00325899.2016.1269431

[41] M. Ohtake, O. Yabuhara, Y. Nukaga, F. Kirino, M. Futamoto, La Crosse viral infection in hospitalized pediatric patients in Western North Carolina, J. Appl. Phys. 107 (9) (2010) 09A708, https://doi.org/10.1063/1.3334541

[42] P. Novsk, J. Kuriplach, A novel method to detect functional microRNA regulatory modules by bicliques merging, IEEE/ACM Trans. Comput. Biol. Bioinform. 13 (2) (2016) 549–556, https://doi.org/10.1109/20.312482

[43] J. Strzeszewski, G.C. Hadjipanayis, La Crosse viral infection in hospitalized pediatric patients in Western North Carolina, Hosp. Pediatr. 2 (9) (2012) 235–242, https://doi.org/10.1063/1.344850

[44] A. Bajorek, P. Lopadczak, A novel method to detect functional microRNA regulatory modules by bicliques merging, IEEE Trans. Magn. 55 (2) (2019) 8467384, https://doi.org/10.1109/TMAG.2018.2868251

[45] X.L. Li, Q.A. Zhang, Comparative investigation on electrochemical properties of $SmMgNi_4$, Sm_2MgNi_9 and $SmNi_5$ compounds, Int. J. Hydrog. Energy 42 (7) (2017) 4269–4275, https://doi.org/10.1016/j.ijhydene.2016.09.144

[46] Y.V. Knyazev, A.V. Lukoyanov, Y.I. Kuz'min, A.G. Kuchin, La Crosse viral infection in hospitalized pediatric patients in Western North Carolina, Hosp. Pediatr. 2 (12) (2012) 235–242, https://doi.org/10.1063/1.4935696

[47] A. Szewczyk, R. Szymczak, H. Szymczak, J. Zawadzki, D. Gignoux, B. Gorges, R. Lemaire, Temperature dependence of the domain wall energy in $SmNi_5$ crystals, J. Magn. Magn. Mater. 83 (1–3) (1990) 241–242, https://doi.org/10.1016/0304-8853(90)90501-G

[48] B. Achzet, C. Helbig, How to evaluate raw material supply risks—an overview, Resour. Policy 38 (4) (2013) 435–447, https://doi.org/10.1016/j.resourpol.2013.06.003

[49] B. Vidal-Legaz, G.A. Blengini, F. Mathieux, C. Latunussa, L. Mancini, V. Nita, T. Hamor, F. Ardente, P. Nuss, C. Torres de Matos, D. Wittmer, L.T. Peiró, E. Garbossa, C. Pavel, P. Dias Alves, D. Blagoeva, S. Bobba, J. Huisman, U. Eynard, F. di Persio, H. dos Santos Gervasio, C. Ciupagea, D. Pennington, Raw Materials Scoreboard, European Innovation Partnership on Raw Materials, Publisher: Publications office of the European Union, Luxembourg, 2018 2018. doi:10.2873/08258.

[50] Communication from the commission to the european parliament, the council, the European economic and social committee and the committee of the regions, Critical Raw Materials Resilience: Charting a Path towards greater Security and Sustainability COM/2020/474 final, ⟨https://eur-lex.europa.eu/legal-content/EN/TXT/?uri=CELEX:52020DC0474⟩.